IJE TRANSACTIONS B: Applications Vol. 34, No. 08, (August 2021) 1827-1836

International Journal of Engineering

Journal Homepage: www.ije.ir

Synergetic Photocatalytic and Adsorptive Removals of Metanil Yellow using TiO_2/Grass-derived Cellulose/Chitosan Film Composite

Rahmi*[a], S. Lubis[a], N. Az-Zahra[a], K. Puspita[b], M. Iqhrammullah[a,c]

[a] *Department of Chemistry, Faculty of Mathematics and Natural Sciences, Universitas Syiah Kuala, Kopelma Darussalam, Indonesia*
[b] *Department of Chemistry Education, Faculty of Education and Teacher Training, Universitas Syiah Kuala, Kopelma Darussalam, Indonesia*
[c] *Graduate School of Mathematics and Applied Sciences, Universitas Syiah Kuala, Kopelma Darussalam, Indonesia*

PAPER INFO

Paper history:
Received 23 April 2021
Received in revised form 16 May 2021
Accepted 04 June 2021

Keywords:
Chitosan
Cellulose
Photocatalyst
Nanoparticle
TiO_2

ABSTRACT

Chitosan (CH) and cellulose are the most abundant biopolymers which could be utilized for hazardous dye removal. By incorporating TiO_2 onto cellulose/CH matrix, our research aimed to achieve high metanil yellow removal by means of synergetic adsorption/photodegradation mechanism. The cellulose particles were extracted from wild grass (*Imperata cylindrica* L.) to obtain grass-derived cellulose (GC). Simple blending method was used to prepare TiO_2/GC/CH, in which the composition was determined by simple additive weighting method (SAW). TiO_2/GC/CH was characterized by means of tensile strength test (also used for SAW), Fourier Transform-Infrared (FT-IR), X-ray diffraction (XRD), differential scanning calorimetry (DSC), and scanning electron microscopy (SEM). Metanil yellow removal using TiO_2/GC/CH works very well at acidic pH range. The removal follows the pseudo-second-order kinetic (R^2 = 0.997) and Langmuir isotherm (R^2 = 0.998) modellings. High q_m obtained from the metanil yellow removal under UV irradiation (q_m = 171.527) proves the synergism between adsorption and photodegradation. The developed TiO_2/GC/CH could be potentially used in the wastewater treatment for azo dye removal.

***doi**: 10.5829/ije.2021.34.08b.03*

1. INTRODUCTION

Chitosan (CH) has been recognized by scientific communities for its excellent properties in removing hazardous contaminants from water, either they are heavy metals or dyes [1, 2]. For practical aspect, CH adsorbent can be prepared in a form of film. In such form, the adsorbent could be easily filtered from the water after the adsorption has been completed. Unfortunately, CH could be easily ruptured by mechanical force and dissolved by acidic solution. To overcome, some studies have prepared CH-based composite using various fillers [3-5].

Cellulose is a good filler candidate, especially because of its high adsorptive performance and rich abundance in nature [6-8]. Some research groups have developed Cellulose/CH-based composite to improve the inherent properties of CH [5, 9, 10]. Our research group focuses on utilizing widely available biomass as the source of cellulose. Previously, we had successfully prepared CH film composite with cellulose derived from oil palm empty fruit bunches [11, 12], and applied it to remove Cd^{2+} from water. Others have used biopolymers as the reinforcement including leaf fibre [13], cassava starch [14], and cellulose [15]. In this research, we used wild grass (*Imperata cylindrica* L.*)* – or locally known as *alang-alang*, as the source for the cellulose filler.

Adsorptive removal could be synergized with photo-induced degradation facilitated by TiO_2 photocatalyst. As a photocatalyst, TiO_2 can be triggered by UV irradiation to produce pairs of electron and holes leading to the generation of hydroxyl radicals [16, 17].

There have been extensive reports regarding the effective photodegradation performed by TiO_2 [18, 19]. Agglomeration is one of the challenges in the

*Corresponding Author Email: rahmi@fmipa.unsyiah.ac.id (Rahmi)

Please cite this article as: Rahmi, S. Lubis, N. Az-Zahra, K. Puspita, and M. Iqhrammullah, Synergetic Photocatalytic and Adsorptive Removals of Metanil Yellow using TiO_2/Grass-derived Cellulose/Chitosan Film Composite, International Journal of Engineering, Transactions B: Applications, Vol. 34, No. 08, (2021) 1827-1836

application of nanoparticles due to the loss of contact surface. Our groups had used TiO_2 for dye removal with various modifications to prevent agglomeration of the nanoparticles [20-22]. Herein, we expected that the cellulose/CH matrix could prevent the agglomeration by fine distribution of the nanoparticles on the matrix surface. Moreover, addition of TiO_2 onto polymeric matrix can improve the physical properties of the material [23, 24].

Indeed, CH, cellulose, and TiO_2 blends have been widely investigated for its performance on removing dyes, but mostly those reported studies used cellulose derivative – cellulose acetate [24-27]. On contrary, we used non-valuable and widely abundant source – grass, as the source to obtain grass-derived cellulose (GC) filler. To test the performance of TiO_2/GC/CH film composite, we chose metanil yellow as a model for azo dye pollutant which occupies 50% of world's dye production [28]. At the end of the day, we expect that our TiO_2/GC/CH film composite can be applied to treat wastewater produced in azo dye-related industries.

2. MATERIALS AND METHODS

2. 1. Materials and Cellulose Extraction Chitosan (CH) as the feed material for the matrix polymer was purchased from Tokyo Chemical Industry Co., Ltd. (Japan) with acetyl degree of 75-85%. Glacial acetic acid, TiO_2 powder, metanil yellow, H_2SO_4, H_2O_2, and pH adjusters (NaOH and HNO_3) were purchased from Sigma-Aldrich (Missouri, United States).

Grass-derived cellulose (GC) had been priorly obtained and its characteristics had been reported [29]. Briefly, powdered grass was hydrolyzed in H_2SO_4 40% and bleached in H_2O_2 30% (at 45°C; 90 min), followed by washing and oven-drying at 40°C.

2. 2. Preparation of TiO_2/GC/CH CH was dissolved in 100 mL glacial acetic acid (20% v/v) and stirred at 250 rpm for 2 h to obtain a matrix solution. GH and TiO_2 were priorly homogenously dispersed in distilled water before they were sequentially added into the matrix solution and stirred at 250 rpm for another 2 and 3 h, respectively. The casting solution was then poured onto a glass mold (17.5 x 12.5 cm) and dried at room temperature for 48 h to obtain the film composite as depicted in Figure 1.

Figure 1. A visual appearance of TiO2/GC/CH composite film

2. 3. Selection of the Best Film Composite To select the best composite we employed simple additive weighting method (SAW) [30]. The decision making analysis was based on the tensile strength of the film and the % removal of metanil yellow, with % priority of 40% and 60%, respectively. Tensile strength was measured by using Universal Testing Machine (UTM) Huang Ta with strain rate of 20 mm/s, where the film's shape followed ASTM D638. Meanwhile, the % removal of metanil yellow from aqueous solution (20 mL) was determined from batch adsorption at equilibrium and pH 6.5 in dark condition using 0.01 g of the film samples, which will be further explained later. Afterward, the data were normalized by dividing each value with the maximum value of all samples. This calculation produced normalized tensile strength (N_a) and normalized removal percentage (N_b). The priority index (Npi) was then calculated by Equation (1):

$$Npi = (40\% \times N_a) + (60\% \times N_b) \quad (1)$$

Film composite with Npi closest to 1 was selected for characterization and further metanil yellow removal studies.

2. 4. Characterization Characterizations of the prepared materials were conducted in Shimadzu Fourier transform – infrared (FT-IR) 8400 (Kyoto, Japan), Jeol. Jsm-6510 LA scanning electron microscope (SEM) (Tokyo, Japan), Shimadzu X-ray diffractometer (XRD)-700 (Kyoto, Japan), and Shimadzu differential scanning calorimetry (DSC)-60 (Kyoto, Japan). The characterization procedures followed our previous reports [6, 31].

2. 5. Batch Adsorption/Photodegradation Metanil yellow removal by TiO_2/GC/CH film composite was conducted (at 250 rpm; 30°C) in two conditions, with and without the presence of UV irradiation for adsorption and synergetic adsorption/photodegradation studies, respectively. The final concentration (Ce (mg/L)) of metanil yellow was calculated employing Shimadzu UV-Vis spectrophotometer (Uvmini-1240, Shimadzu, Kyoto, Japan) at λ_{max} = 432 nm after the pH adjustment into 6, as suggested previously [32]. For the contact time studies, the procedure was carried out at pH 6.5 using 0.05 g TiO_2/GC/CH in 25 mL metanil yellow (100 mg/L). The adsorption parameters followed the suggestion of previous reports [33, 34]. All the following studies employed the optimum adsorption parameters obtained earlier (100 minutes contact time; pH 3). Adsorption capacity at *t* time (q_t (mg/g)), adsorption capacity at equilibrium (q_e (mg/g)), and removal percentage (%) were calculated based on the equations we had used in the previous reports [35-37]. For the photodegradatino using UV irradiation, a UV lamp (6 W; λ = 365 nm) was used and positioned 10 cm away from the batch container.

3. RESULTS AND DISCUSSION

3. 1. Effect of Filler Addition on the Tensile Strength and Metanil Yellow Uptake Addition of GC and TiO_2 promotes adhesive force, resulting in higher tensile strength than neat CH (Table 1). The addition of fillers prevents the slipping effect and reduces the void in the matrix. Our findings are consistent with the previously reported studies [3, 4, 38, 39].

However, adverse effect of GC and TiO_2 fillers incorporation onto chitosan matrix on metanil yellow removal was observed. It is presumably because of the blockage of the binding sites in the chitosan. Yet, TiO_2 embedment was expected to provide synergetic adsorptive and photocatalytic removal. In determining the optimum composite, the removal was merely based on the adsorption since it was conducted in dark condition.

The aim of preparing this composite is not only to obtain a material that performs the highest dye removal. For practical purposes, the composite film should possess a good endurance against mechanical stress from the water flow. Therefore, mechanical properties of the material should also be taken into account. Combinations of TiO_2, GC, and CH yield complex interaction, resulting in unpredictable tensile strength and metanil yellow removal performance. Therefore, selection of the most optimum composite was determined through SAW method, where composite with the composition of 0.9 g CH, 0.05 g GC, and 0.05 g TiO_2 was selected due to its possession of the highest Npi value (Table 1).

3. 2. Characteristics The purposes of analyzing FT-IR spectra (Figure 2) are: a) Investigating the success of GC and TiO_2 fillers addition, and b) Identifying functional groups that can act as active sites, namely O- and N-containing groups [35, 40]. Overlapping of O-H and N-H stretching vibration was observed at a range of around 3500 – 3000 cm^{-1} in all samples. Within the same wavenumber range, GC/CH and TiO_2/GC/CH showed broader spectral bands indicating the addition of O-H from GC [41] and $TiO(OH)_2$ nanoparticles [42]. Amide I bands (N-H deformation and C-O stretching) of typical CH were observed at 1638 cm^{-1}; shifted to lower wavenumber 1632 cm^{-1} stem from the effect of GC and TiO_2 addition. Transmittance peaks at1147 and 888 cm^{-1} from CH are assigned to C-O-C and C=O stretching, respectively. These peaks were shifted to higher wavenumber associated with the successful immobilization of GC and TiO_2 [43, 44]. The immobilization of TiO_2 into GC/CH could also be proven by the appearance of transmittance peak of O-Ti-O stretching vibration, which is similar to the previously reported study [45].

Based on the diffractogram of CH (Figure 3a), the appearance of amorphous peak at $2\theta = 20.00°$ is typical for hydrophilic chitosan crystalline lattice [46]. Previously, GC had been characterized using XRD where the typical peaks at 15.24° and 21.96° (2θ) were found [46]. In this study, those peaks were not observable in GC/CH composite. Moreover, the addition of GC resulted in the disappearance of several peaks in CH matrix (2θ = 37.79, 57.90, 64.73, and 77.68), indicating the change in polymer crystallinity. A new peak at 24.85 in TiO_2/GC/CH corresponds to the immobilization of TiO_2. Significant decrease at 20.00° (2θ) in GC/CH and TiO_2/GC/CH is ascribed to the addition of those GC and TiO_2 as fillers. Depression of crystalline lattice of CH may occur due to the presence of those fillers induced by both hydrogen bonds and steric effect [45]. It is then confirmed by quantitatively calculate the crystallinity of the samples using the proposed method [12, 47]; crystalline peaks divided by noises of the entire diffractogram and multiplied by

TABLE 1. Results of SAW analysis based on the tensile strength and q_e

Composition	Criteria		Npi
	Tensile Strength (kgf/mm^2)	Removal (%)	
CH (1 g)	12.33	99.07	0.90
CH : GC (0.9 g : 0.1 g)	14.00	98.82	0.94
CH : TiO_2 (0.9 g : 0.1 g)	15.42	98.88	0.98
CH : GC : TiO_2 (0.9 g : 0.025 g : 0.075 g)	14.25	99.13	0.95
CH : GC : TiO_2^* (0.9 g : 0.05 g : 0.05 g)	16.17	98.80	1.00
CH : GC : TiO_2 (0.9 g : 0.075 g : 0.025 g)	14.25	99.04	0.95

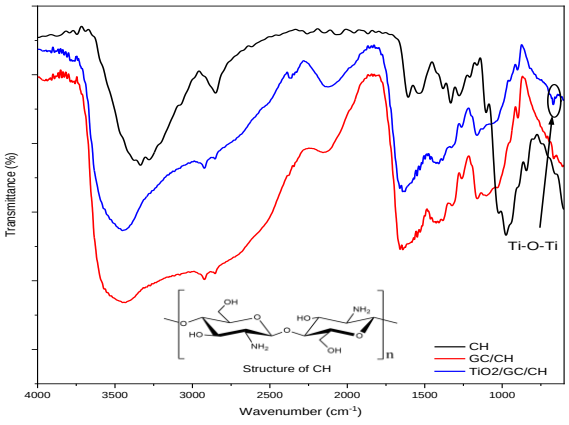

Figure 2. FT-IR spectra of CH, GC/CH, and TiO_2/GC/CH

100%. CH, GC/CH, and TiO_2/GC/CH have crystallinity indices of 63.86%, 30.32%, and 27.96%, respectively.

DSC analysis aims to see the endothermic and exothermic temperatures of the chitosan-cellulose-TiO_2 composite film, which in principle measures the difference in heat that enters with that of reference temperature. Endothermic shoulder at 115.67°C in CH thermogram (Figure 3b) is ascribed to the presence of water evaporation, where higher temperature was needed to evaporate the water in GC (T_{peak} = 156.36°C). It is probably due to the higher hydrophilicity of GC, as opposed to CH, resulting in stronger binding of water molecules. Interestingly, the endothermic shoulder return to lower temperature after the embedment of TiO_2. There have been reports where TiO_2 embedment can increase the hydrophobicity of a material [48, 49].

Exothermic peak at 338.97°C is ascribed to the decomposition of CH, whereas in GC/CH and TiO_2/GC/CH, the decomposition was observed by two identical exothermic peaks (at 319 and 395°C). The thermal profile of GC/CH with two exothermic decomposition peaks explains two different polymers in the composites (GC and CH). The inherent decomposition temperature of CH decreased in the composite, which can be attributed to the reduction of intermolecular interaction of chitosan caused by the presence of GC particles. It is corroborated by the XRD thermogram, where GC addition resulted in the deformation of CH crystalline structure. Meanwhile, the addition of TiO_2 appeared to contribute to slower decomposition, where broader exothermic peak at 395°C is observed and ascribed to the degradation of not only the polysaccharide and but also the O-H from TiO_2 [43].

SEM images of CH, GC, GC/CH, and TiO_2/GC/CH (Figure 4) are used to examine the surface morphology of the samples. SEM image of CH shows a smooth surface which indicates its homogenous mixing in the solvent – in line with a previously reported study [50]. Diverse sizes of GC particles are observed with fibrous shape and a diameter of 10 to 50 µm. The difference may be influenced by the hydrolysis and bleaching process. GC/CH composite is observed to be having rougher surface than CH. From the image, we can see that GC was totally enveloped with CH layer indicating the compatible composite. TiO_2 nanoparticles can be observed to be very well dispersed on the GC/CH surface, suggesting the successful embedment polymer [25]. However, several agglomerations of TiO_2 were observed as shown by the red arrow.

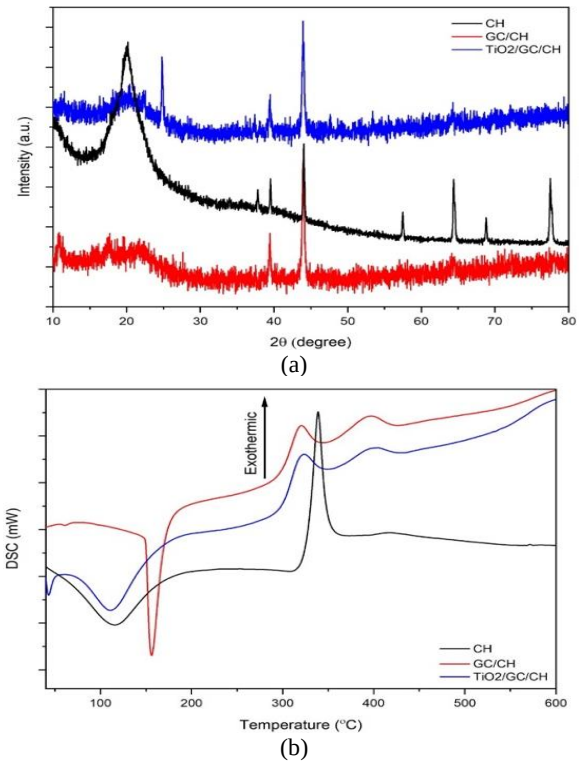

Figure 3. XRD patterns and DSC thermogram of CH, GC/CH, and TiO_2/GC/CH

3. 3. Metanil Yellow Removal

3. 3. 1. Optimum Adsorption Parameters

Two important parameters for metanil yellow removal via adsorption or photodegradation, namely contact time and pH, had been studied (Figure 4). Rapid increment of the adsorption capacities from the 20th to 60th minute

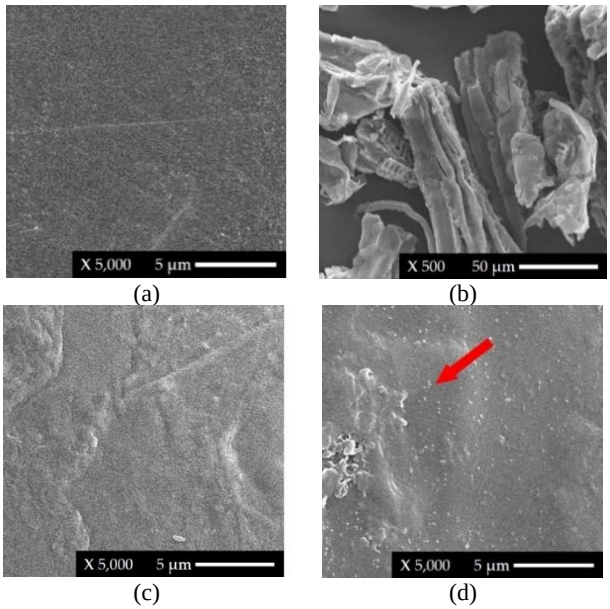

Figure 4. SEM images of (a) CH film, (b) GC particles, (c) GC/CH film, and (d) TiO_2/GC/CH film with 5,000 x magnification. The red arrow indicated the presence of TiO_2 agglomeration.

was observed to be 135% and 202% for the adsorption and adsorption/photodegradation, respectively (Figure 5a). It is due to the high diffusion force as at the initial phase, the vacant binding sites is still numerous. On contrary, at longer contact time the adsorption is governed by chemical interaction between adsorbate and adsorbent surface. Higher adsorption capacity from the adsorption/photodegradation, especially at 60th minute, may indicate the synergetic mechanism. However, further studies using isothermal modelling were used to substantiate the synergism. As the metanil yellow pollutant attaches to the TiO_2/GC/CH surface, the pollutant will be photodegraded by TiO_2 – providing extra vacant site. This process reached equilibrium at 100th minute indicated by the saturation of adsorption capacity in the following contact times. At equilibrium, the adsorption capacity for adsorption and adsorption/photodegradation were 47.84 and 48.28 mg/g, respectively. Therefore, the following investigations were carried out for 100 minutes.

Metanil yellow is an acid dye which forms negative ions in aqueous solution – anionic dye [51]. When the anionic dye interacted with positively charged adsorbent, the adsorption would increase due to electrostatic interaction between the opposite charges.

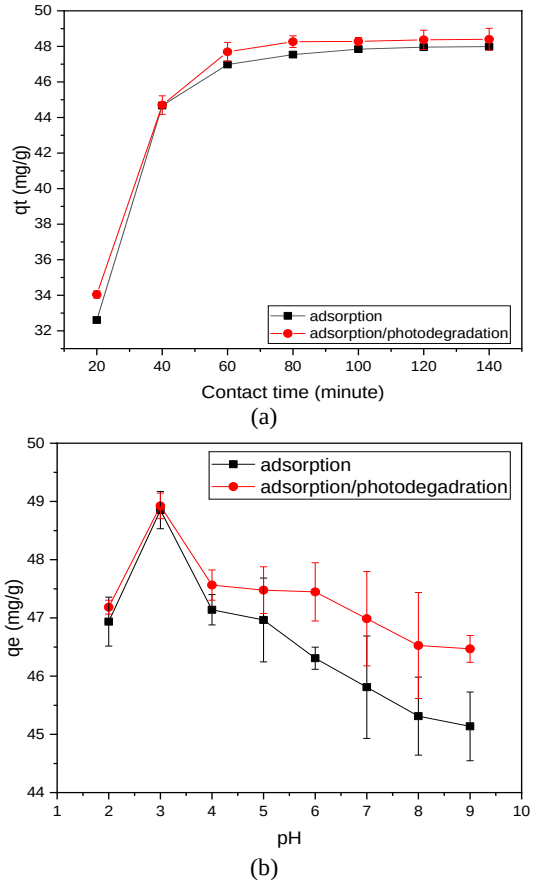

Figure 5. Effects of (a) contact time and (b) pH on the removal of metanil yellow by TiO_2/GC/CH film composite

When pH > 3, the adsorption capacity of metanil yellow decreased reciprocally with the increase of pH (Figure 5b). It stems from the fact that CH matrix from TiO_2/GC/CH composite was protonated in acidic solution producing positively charged surface [51, 52]. Furthermore, in acidic solution, TiO_2 may produce hydroxyl radicals via hole trapping mechanism [16, 53]. Nonetheless, at high pH value, the adsorption/photodegradation process performed higher adsorption capacity than the adsorption alone. It suggests that at high pH, the removal was not only dependant on the electrostatic attraction-based adsorption, but rather on the photodegradation mechanism. In basic solution, the formation of $OH^{\bullet}$ can still occur via electroreduction of dissolved O_2 [16, 53]. Therefore, the working pH range can be broadened by incorporating TiO_2 which can benefit the removal process without decreasing the solution pH, in addition to its practical aspect. However, since pH 3 facilitated the highest removal of metanil yellow, the pH value was selected for further investigations.

3. 3. 2. Kinetic and Isotherm Studies The adsorptive behavior of methanyl yellow using TiO_2/GC/CH composite film was investigated by the kinetic modeling. Therefore, two kinetic models were employed, namely pseudo-first-order (Equations (2)) and pseudo-second-order (Equation (3)), as used in previous studies [23, 40].

$$\log(q_e - q_t) = \log q_e - \frac{k_1}{2.303} t \quad (2)$$

$$\frac{t}{q_t} = \frac{1}{k_2 q_e^2} + \frac{t}{q_e} \quad (3)$$

where k_1 and k_2 are the constant rate of pseudo-first-order and pseudo-second-order, respectively.

Kinetic model for adsorption and adsorption/photodegradation of metanil yellow using TiO_2/GC/CH has been presented based on the linear equations of pseudo-first-order (Figure 6a) and pseudo-second-order (Figure 6b). The adsorption and adsorption/photodegradation fit the pseudo-second-order equation the most with R^2 = 0.997 and 0.9975, respectively (Table 2).

Another statistical parameter that could be considered is the values of Root-Mean-Square-Errors (RMSE) that are lower in pseudo-second-order. Thus, we concluded that the adsorption and adsorption/photodegradation follows the assumption of pseudo-second-order, in which the rate-limiting step depends on the chemisorption [40, 54]. Nonetheless, since the data solely rely on the modelling approach, we suggest further study to confirm the chemisorption dominance.

Isotherm modellings were used to study the interaction phenomenon in the adsorption and

TABLE 2. Kinetic parameters for adsorption and adsorption/photodegradation of metanil yellow using TiO_2/GC/CH.

Kinetic models	Parameters	Adsorption	Adsorption/ photodegradation
Pseudo-first-order	R^2	0.98856	0.95852
	RMSE	0.10349	0.20684
	K_1 (g/mg.min)	0.0593	0.0615
	q_e (mg/g)	43.1728	37.3534
Pseudo-second-order	R^2	0.99699	0.9975
	RMSE	0.04638	0.04206
	K_1 (g/mg.min)	0.0026	0.0028
	q_e (mg/g)	51.2033	51.3611

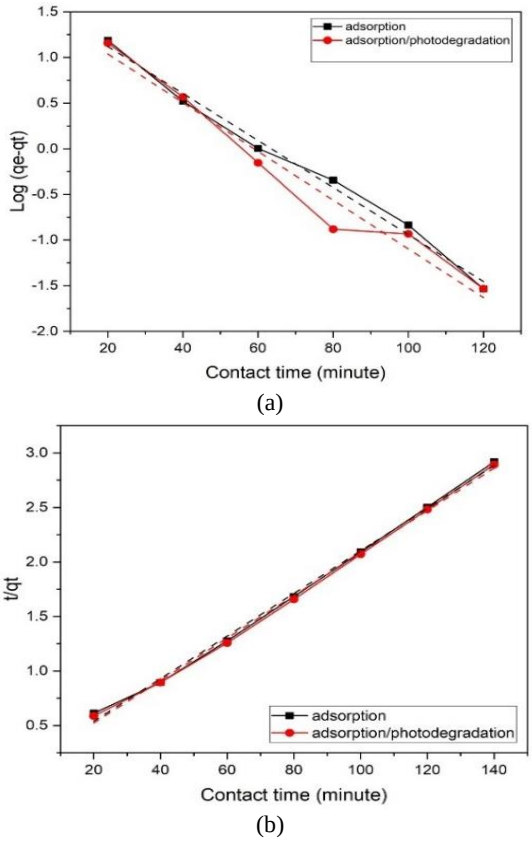

Figure 6. Kinetic modelling with (a) pseudo-first-order and (b) pseudo-second-order equations for metanil yellow removal using TiO_2/GC/CH film composite

adsorption-photodegradation process. Herein, we employed the common Langmuir and Freundlich isotherm models. The linearized equations for Langmuir (Equation (3)) and Freundlich (Equation (4)) are shown below:

$$\frac{1}{q_e} = \frac{1}{q_m} + \frac{1}{K_L q_m c_e} \quad (4)$$

$$Log\ q_e = Log\ K_F + \frac{1}{n} Log\ C_e \quad (5)$$

These equations have been used in the previous works [7, 55], where q_m (mg/g) is the maximum adsorption capacity, K_L is Langmuir constant, and K_F and *n* are Freundlich constants. K_L and K_F represent the free energy and removal capacity, respectively, meanwhile *n* is for adsorption intensity.

The isotherm modellings of metanil yellow removal via adsorption and adsorption/photodegradation based on linearized Langmuir (Figure 6a) and Freundlich (Figure 6b) equations have been presented. The study revealed that both adsorption and adsorption/photodegradation of metanil yellow in our work are Langmuir-dependent with R^2 = 0.998 and 0.9865, respectively (Table 3).

The RMSE are also 7.5 and 5 times lower in Langmuir than in Freundlich modelling for the adsorption and adsorption/photodegradation, respectively. Therefore, the adsorptive interaction between metanil yellow and TiO_2/GC/CH, either with or

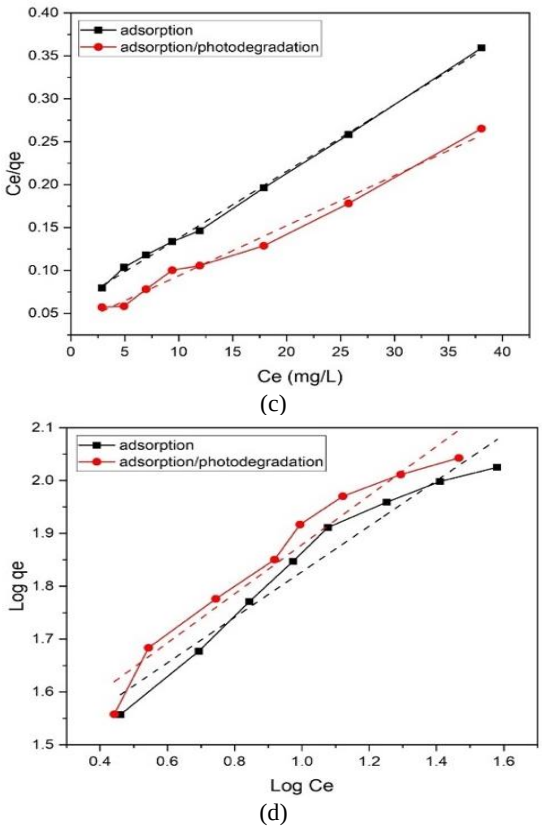

Figure 7. isotherm modelling with (a) Langmuir and (b) Freundlich equations for metanil yellow removal using TiO_2/GC/CH film composite

TABLE 3. Isotherms parameters for adsorption and adsorption-photodegradation of metanil yellow using TiO_2/GC/CH.

Kinetic models	Parameters	Adsorption	Adsorption/ photodegradation
Langmuir	R^2	0.99786	0.98649
	RMSE	0.00432	0.00817
	K_L (L/mg)	0.1299	0.1628
	q_m (mg/g)	128.5347	171.5266
Freundlich	R^2	0.94663	0.94114
	RMSE	0.03807	0.04108
	K_F (mg/g)	24.917	25.939
	n	2.320	2.152

without light exposure, follows the assumptions that each active site shares the same binding energy and the adsorption occurs in monolayer.

Maximum adsorption capacity from the Langmuir equation revealed that the metanil yellow removal via adsorption has a higher value (128.5347 mg/g) as opposed to that of adsorption/photodegradation (171.527 mg/g). Neat TiO_2 nano powder is reported to have $q_m = 2.79 \times 10^{-4}$ mg/g [18], which is far smaller compared with TiO_2/GC/CH in our work. It confirms that the higher q_m was obtained due to the synergism between adsorption and photodegradation in reducing the level of metanil yellow from water. Comparatively, other studies have used chitosan-based adsorbent and achieved higher q_m for metanil yellow adsorption. A research group led by Tural has accomplished $q_m = 625$ mg/g [32], Tehrani-Bagha with $q_m = 910$ mg/g [56], and Lee with $q_m = 558.18$ mg/g [57]. But they used adsorbents in a form of nanoparticles [32, 56] and aerogels [57] which are less practical than film adsorbent due to their separation difficulty. Additionally, the Langmuir constants of more than 0.01 (0.132 and 0.239 for adsorption and adsorption/photodegradation, respectively) can be associated with intense adsorbate-adsorbent interaction [58].

4. CONCLUSION

We have successfully prepared TiO_2/GC/CH with improved mechanical properties and synergetic adsorption/photodegradation ability for metanil yellow removal. Characterization using FT-IR proves the successful attachment of TiO_2 onto GC/CH matrix and the presence of N- and O-containing groups. Through XRD analysis, we have observed the loss of crystallinity of CH upon the addition of TiO_2 nanoparticles and GC particles. SEM images confirm the distribution of embedded TiO_2 nanoparticles on the GC/CH, with the presence of several agglomerations. DSC analysis revealed that GC addition can increase bonding intensity between water molecules and adsorbents, while TiO_2 reduce the bonding intensity. The performance in metanil yellow removal suggests the synergetic adsorption and photodegradation mechanism of TiO_2/GC/CH that follows pseudo-second-order kinetic and Langmuir isotherm modellings. Additionally, the role of TiO_2 photocatalyst can broaden the working pH range for the metanil yellow removal which improves the practical aspect of our material. However, the agglomeration was still a challenge in this study which might be responsible for the low photodegradation activities.

5. REFERENCES

1. Zhang, L., Zeng, Y. and Cheng, Z., "Removal of heavy metal ions using chitosan and modified chitosan: A review", ***Journal of Molecular Liquids***, Vol. 214, (2016), 175-191. DOI: 10.1016/j.molliq.2015.12.013.
2. Vakili, M., Deng, S., Cagnetta, G., Wang, W., Meng, P., Liu, D. and Yu, G., "Regeneration of chitosan-based adsorbents used in heavy metal adsorption: A review", ***Separation and Purification Technology***, Vol. 224, (2019), 373-387. DOI: 10.1016/j.seppur.2019.05.040.
3. Kavimani, V., Soorya Prakash, K., Thankachan, T. and Udayakumar, R., "Synergistic improvement of epoxy derived polymer composites reinforced with graphene oxide (GO) plus titanium di oxide(TiO_2)", ***Composites Part B: Engineering***, Vol. 191, (2020). DOI: 10.1016/j.compositesb.2020.107911.
4. Shirkavand, S. and Moslehifard, E., "Effect of TiO_2 nanoparticles on tensile strength of dental acrylic resins", ***Journal of Dental Research, Dental Clinics, Dental Prospects***, Vol. 8, No. 4, (2014), 197-203. DOI: 10.5681/joddd.2014.036.
5. Valizadeh, S., Naseri, M., Babaei, S., Hosseini, S.M.H. and Imani, A., "Development of bioactive composite films from chitosan and carboxymethyl cellulose using glutaraldehyde, cinnamon essential oil and oleic acid", ***International Journal of Biological Macromolecules***, Vol. 134, (2019), 604-612. DOI: 10.1016/j.ijbiomac.2019.05.071.
6. Iqhrammullah, M., Marlina, M., Khalil, H., Kurniawan, K.H., Suyanto, H., Hedwig, R., Karnadi, I., Olaiya, N.G., Abdullah, C.K. and Abdulmadjid, S.N., "Characterization and performance evaluation of cellulose acetate-polyurethane film for lead II ion removal", ***Polymers (Basel)***, Vol. 12, No. 6, (2020). DOI: 10.3390/polym12061317.
7. Santoso, S.P., Kurniawan, A., Soetaredjo, F.E., Cheng, K.-C., Putro, J.N., Ismadji, S. and Ju, Y.-H., "Eco-friendly cellulose–bentonite porous composite hydrogels for adsorptive removal of azo dye and soilless culture", ***Cellulose***, Vol. 26, No. 5, (2019), 3339-3358. DOI: 10.1007/s10570-019-02314-2.
8. Shen, S.S., Yang, J.J., Liu, C.X. and Bai, R.B., "Immobilization of copper ions on chitosan/cellulose acetate blend hollow fiber membrane for protein adsorption", ***RSC Advances***, Vol. 7, No. 17, (2017), 10424-10431. DOI: 10.1039/c7ra00148g.
9. Alni, A., Puspita, K. and Zulfikar, M.A., "Biosorbent from chinese cabbage (*Brassica pekinensia* L.) for phenol contaminated waste water treatment", ***Key Engineering***

Materials, Vol. 811, (2019), 71-79. DOI: 10.4028/www.scientific.net/KEM.811.71.

10. Zheng, X., Li, X., Li, J., Wang, L., Jin, W., Liu, J., Pei, Y. and Tang, K., "Efficient removal of anionic dye (congo red) by dialdehyde microfibrillated cellulose/chitosan composite film with significantly improved stability in dye solution", ***International Journal of Biological Macromolecules***, Vol. 107, No. Pt A, (2018), 283-289. DOI: 10.1016/j.ijbiomac.2017.08.169.
11. Rahmi, Lelifajri, Julinawati and Shabrina, "Preparation of chitosan composite film reinforced with cellulose isolated from oil palm empty fruit bunch and application in cadmium ions removal from aqueous solutions", ***Carbohydrate Polymers***, Vol. 170, (2017), 226-233. DOI: 10.1016/j.carbpol.2017.04.084.
12. Rahmi, Iqhrammullah, M., Audina, U., Husin, H. and Fathana, H., "Adsorptive removal of Cd (ii) using oil palm empty fruit bunch-based charcoal/chitosan-edta film composite", ***Sustainable Chemistry and Pharmacy***, Vol. 21, (2021). DOI: 10.1016/j.scp.2021.100449.
13. Jumaidin, R., Diah, N.A., Ilyas, R.A., Alamjuri, R.H. and Yusof, F.A.M., "Processing and characterisation of banana leaf fibre reinforced thermoplastic cassava starch composites", ***Polymers (Basel)***, Vol. 13, No. 9, (2021). DOI: 10.3390/polym13091420.
14. Jumaidin, R., Khiruddin, M.A.A., Asyul Sutan Saidi, Z., Salit, M.S. and Ilyas, R.A., "Effect of cogon grass fibre on the thermal, mechanical and biodegradation properties of thermoplastic cassava starch biocomposite", ***International Journal of Biological Macromolecules***, Vol. 146, (2020), 746-755. DOI: 10.1016/j.ijbiomac.2019.11.011.
15. Omran, A.A.B., Mohammed, A., Sapuan, S.M., Ilyas, R.A., Asyraf, M.R.M., Rahimian Koloor, S.S. and Petru, M., "Micro- and nanocellulose in polymer composite materials: A review", ***Polymers (Basel)***, Vol. 13, No. 2, (2021). DOI: 10.3390/polym13020231.
16. Schneider, J., Matsuoka, M., Takeuchi, M., Zhang, J., Horiuchi, Y., Anpo, M. and Bahnemann, D.W., "Understanding TiO_2 photocatalysis: Mechanisms and materials", ***Chemical Reviews***, Vol. 114, No. 19, (2014), 9919-9986. DOI: 10.1021/cr5001892.
17. Rostami, M., Joshaghani, A.H., Mazaheri, H. and Shokri, A., "Photo-degradation of p-nitro toluene using modified bentonite based nano-TiO_2 photocatalyst in aqueous solution", ***International Journal of Engineering***, Vol. 34, No. 4, (2021), 756-762. DOI: 10.5829/IJE.2021.34.04A.01.
18. Chakrabortty, D. and Sen Gupta, S., "Decolourisation of metanil yellow by visible-light photocatalysis with n-doped TiO_2 nanoparticles: Influence of system parameters and kinetic study", ***Desalination and Water Treatment***, Vol. 52, No. 28-30, (2013), 5528-5540. DOI: 10.1080/19443994.2013.808594.
19. Nguyen, C.H., Tran, M.L., Tran, T.T.V. and Juang, R.-S., "Enhanced removal of various dyes from aqueous solutions by UV and simulated solar photocatalysis over TiO2/ZnO/RGO composites", ***Separation and Purification Technology***, Vol. 232, (2020). DOI: 10.1016/j.seppur.2019.115962.
20. Irwan, I., Lubis, S., Ramli, M. and Sheilatina, S., "Photocatalytic degradation of indigo carmine by TiO_2/activated carbon derived from waste coffee grounds", ***Journal Natural***, Vol. 16, No. 1, (2016), 21-26. DOI: 10.24815/jn.v16i1.4640.
21. Lubis, S., Sheilatina and Murisna, "Synthesis, characterization and photocatalytic activity of α-fe_2o_3/bentonite composite prepared by mechanical milling", ***Journal of Physics: Conference Series***, Vol. 1116, (2018). DOI: 10.1088/1742-6596/1116/4/042016.
22. Lubis, S., Maulana, I. and Masyithah, "Synthesis and characterization of TiO_2/α-Fe_2O_3 composite using hematite from iron sand for photodegradation removal of dye", ***Journal Natural***, Vol. 18, No. 1, (2018), 38-43. DOI: 10.24815/jn.v18i1.8649.
23. Razzaz, A., Ghorban, S., Hosayni, L., Irani, M. and Aliabadi, M., "Chitosan nanofibers functionalized by tio_2 nanoparticles for the removal of heavy metal ions", ***Journal of the Taiwan Institute of Chemical Engineers***, Vol. 58, (2016), 333-343. DOI: 10.1016/j.jtice.2015.06.003.
24. Shi, X., Zhang, X., Ma, L., Xiang, C. and Li, L., "TiO_2-doped chitosan microspheres supported on cellulose acetate fibers for adsorption and photocatalytic degradation of methyl orange", ***Polymers (Basel)***, Vol. 11, No. 8, (2019). DOI: 10.3390/polym11081293.
25. Mafirad, S., Mehrnia, M.R., Zahedi, P. and Hosseini, S.N., "Chitosan-based nanocomposite membranes with improved properties: Effect of cellulose acetate blending and TiO_2 nanoparticles incorporation", ***Polymer Composites***, Vol. 39, No. 12, (2017), 4452-4466. DOI: 10.1002/pc.24539.
26. Yu, H., Liu, H., Yuan, X., Ding, W., Li, Y. and Wang, J., "Separation of oil-water emulsion and adsorption of Cu(II) on a chitosan-cellulose acetate-TiO_2 based membrane", ***Chemosphere***, Vol. 235, (2019), 239-247. DOI: 10.1016/j.chemosphere.2019.06.060.
27. ZabihiSahebi, A., Koushkbaghi, S., Pishnamazi, M., Askari, A., Khosravi, R. and Irani, M., "Synthesis of cellulose acetate/chitosan/SWCNT/Fe_3O_4/TiO_2 composite nanofibers for the removal of Cr(VI), As(V), methylene blue and congo red from aqueous solutions", ***International Journal of Biological Macromolecules***, Vol. 140, (2019), 1296-1304. DOI: 10.1016/j.ijbiomac.2019.08.214.
28. Chung, K.T., "Azo dyes and human health: A review", ***Journal of Environmental Science and Health, Part C: Toxicology and Carcinogenesis***, Vol. 34, No. 4, (2016), 233-261. DOI: 10.1080/10590501.2016.1236602.
29. Az-Zahra, N., Rahmi, R. and Lubis, S., "Reinforcement of chitosan film using cellulose isolated from grass (*Imperata cylindrica*)", ***Journal of Physics: Conference Series***, Vol. 1402, (2019). DOI: 10.1088/1742-6596/1402/5/055039.
30. Hwang, C.-L. and Yoon, K., "Multiple attribute decision making, Lecture notes in economics and mathematical systems, Berlin, Heidelberg, Springer Berlin Heidelberg, Vol. 186, (1981). DOI: 10.1007/978-3-642-48318-9.
31. Rahmi, Lelifajri and Nurfatimah, R., "Preparation of polyethylene glycol diglycidyl ether (PEDGE) crosslinked chitosan/activated carbon composite film for Cd^{2+} removal", ***Carbohydrate Polymers***, Vol. 199, (2018), 499-505. DOI: 10.1016/j.carbpol.2018.07.051.
32. Tural, S., Tarhan, T. and Tural, B., "Removal of hazardous azo dye metanil yellow from aqueous solution by cross-linked magnetic biosorbent; equilibrium and kinetic studies", ***Desalination and Water Treatment***, Vol. 57, No. 28, (2015), 13347-13356. DOI: 10.1080/19443994.2015.1056842.
33. Davarnejad, R. and Karimi Dastnayi, Z., "Cd (II) removal from aqueous solutions by adsorption on henna and henna with chitosan microparticles using response surface methodology", ***Iranian Journal of Chemistry and Chemical Engineering***, Vol. 38, No. 3, (2019), 267-281. DOI: 10.30492/IJCCE.2019.30929.
34. Davarnejad, R., Karimi Dastnayi, Z. and Kennedy, J.F., "Cr(VI) adsorption on the blends of henna with chitosan microparticles: Experimental and statistical analysis", ***International Journal of Biological Macromolecules***, Vol. 116, (2018), 281-288. DOI: 10.1016/j.ijbiomac.2018.04.189.
35. Marlina, Iqhrammullah, M., Saleha, S., Fathurrahmi, Maulina, F.P. and Idroes, R., "Polyurethane film prepared from ball-milled algal polyol particle and activated carbon filler for NH_3-N

removal", ***Heliyon***, Vol. 6, No. 8, (2020), e04590. DOI: 10.1016/j.heliyon.2020.e04590.

36. Rahmi, Fathurrahmi, Lelifajri and PurnamaWati, F., "Preparation of magnetic chitosan using local iron sand for mercury removal", ***Heliyon***, Vol. 5, No. 5, (2019), e01731. DOI: 10.1016/j.heliyon.2019.e01731.
37. Arahman, N., Fitri, R.A., Wirakusuma, A., Fahrina, A. and Bilad, M.R., "Adsorption performance of low-cost java plum leaves and guava fruits as natural adsorbents for removal of free fatty acids from coconut oil", ***International Journal of Engineering***, Vol. 32, No. 10, (2019), 1372-1378. DOI: 10.5829/ije.2019.32.10a.06.
38. Guo, S.-Y., Zhang, X., Ren, J., Chen, J.-Z., Zhao, T.-J., Li, T.-W. and Zhang, L., "Preparation of tio$_2$/epoxy resin composite and its effect on mechanical and bonding properties of opc mortars", ***Construction and Building Materials***, Vol. 272, (2021). DOI: 10.1016/j.conbuildmat.2020.121960.
39. Vosough, M., Sharafi, S. and Khayati, G.R., "Co-tio$_2$ nanoparticles as the reinforcement for fe soft magnetic composites with enhanced mechanical and magnetic properties via pulse electrodeposition", ***International Journal of Engineering***, Vol. 33, No. 10, (2020), 2030-2038. DOI: 10.5829/ije.2020.33.10a.21.
40. Iqhrammullah, M., Marlina and Nur, S., "Adsorption behaviour of hazardous dye (methyl orange) on cellulose-acetate polyurethane sheets", ***IOP Conference Series: Materials Science and Engineering***, Vol. 845, (2020). DOI: 10.1088/1757-899x/845/1/012035.
41. Luzi, F., Puglia, D., Sarasini, F., Tirillo, J., Maffei, G., Zuorro, A., Lavecchia, R., Kenny, J.M. and Torre, L., "Valorization and extraction of cellulose nanocrystals from North African grass: *Ampelodesmos mauritanicus* (diss)", ***Carbohydrate Polymers*** Vol. 209, (2019), 328-337. DOI: 10.1016/j.carbpol.2019.01.048.
42. León, A., Reuquen, P., Garín, C., Segura, R., Vargas, P., Zapata, P. and Orihuela, P., "FTIR and Raman characterization of TiO_2 nanoparticles coated with polyethylene glycol as carrier for 2-methoxyestradiol", ***Applied Sciences***, Vol. 7, No. 1, (2017). DOI: 10.3390/app7010049.
43. Behera, S.S., Das, U., Kumar, A., Bissoyi, A. and Singh, A.K., "Chitosan/TiO_2 composite membrane improves proliferation and survival of l929 fibroblast cells: Application in wound dressing and skin regeneration", ***International Journal of Biological Macromolecules***, Vol. 98, (2017), 329-340. DOI: 10.1016/j.ijbiomac.2017.02.017.
44. Terán, E.J., Montes, M.L., Rodríguez, C., Martino, L., Quiroga, M., Landa, R., Torres Sánchez, R.M. and Díaz Pace, D.M., "Assessment of sorption capability of montmorillonite clay for lead removal from water using laser–induced breakdown spectroscopy and atomic absorption spectroscopy", ***Microchemical Journal***, Vol. 144, (2019), 159-165. DOI: 10.1016/j.microc.2018.08.047.
45. Montaser, A.S., Wassel, A.R. and Al-Shaye'a, O.N., "Synthesis, characterization and antimicrobial activity of schiff bases from chitosan and salicylaldehyde/tio2 nanocomposite membrane", ***International Journal of Biological Macromolecules***, Vol. 124, (2019), 802-809. DOI: 10.1016/j.ijbiomac.2018.11.229.
46. Tsai, H.-S. and Wang, Y.-Z., "Properties of hydrophilic chitosan network membranes by introducing binary crosslink agents", ***Polymer Bulletin***, Vol. 60, No. 1, (2007), 103-113. DOI: 10.1007/s00289-007-0846-x.
47. de Queiroz Antonino, R., Lia Fook, B.R.P., de Oliveira Lima, V.A., de Farias Rached, R.I., Lima, E.P.N., da Silva Lima, R.J., Peniche Covas, C.A. and Lia Fook, M.V., "Preparation and characterization of chitosan obtained from shells of shrimp (*Litopenaeus vannamei boone*)", ***Marine Drugs***, Vol. 15, No. 5, (2017). DOI: 10.3390/md15050141.
48. Li, C., Sun, Y., Cheng, M., Sun, S. and Hu, S., "Fabrication and characterization of a TiO_2/polysiloxane resin composite coating with full-thickness super-hydrophobicity", ***Chemical Engineering Journal***, Vol. 333, (2018), 361-369. DOI: 10.1016/j.cej.2017.09.165.
49. Lou, L., Kendall, R.J. and Ramkumar, S., "Comparison of hydrophilic PVA/TiO_2 and hydrophobic PVDF/TiO_2 microfiber webs on the dye pollutant photo-catalyzation", ***Journal of Environmental Chemical Engineering***, Vol. 8, No. 5, (2020). DOI: 10.1016/j.jece.2020.103914.
50. Salari, M., Sowti Khiabani, M., Rezaei Mokarram, R., Ghanbarzadeh, B. and Samadi Kafil, H., "Preparation and characterization of cellulose nanocrystals from bacterial cellulose produced in sugar beet molasses and cheese whey media", ***International Journal of Biological Macromolecules***, Vol. 122, (2019), 280-288. DOI: 10.1016/j.ijbiomac.2018.10.136.
51. Guo, X., Wei, Q., Du, B., Zhang, Y., Xin, X., Yan, L. and Yu, H., "Removal of metanil yellow from water environment by amino functionalized graphenes (NH_2-G) – influence of surface chemistry of NH_2-G", ***Applied Surface Science***, Vol. 284, (2013), 862-869. DOI: 10.1016/j.apsusc.2013.08.023.
52. Santra, A.K., Pal, T.K. and Datta, S., "Removal of metanil yellow from its aqueous solution by fly ash and activated carbon produced from different sources", ***Separation Science and Technology***, Vol. 43, No. 6, (2008), 1434-1458. DOI: 10.1080/01496390701885729.
53. Hoffmann, M.R., Martin, S.T., Choi, W. and Bahnemann, D.W., "Environmental applications of semiconductor photocatalysis", ***Chemical Reviews***, Vol. 95, No. 1, (2002), 69-96. DOI: 10.1021/cr00033a004.
54. Robati, D., Mirza, B., Rajabi, M., Moradi, O., Tyagi, I., Agarwal, S. and Gupta, V.K., "Removal of hazardous dyes-br 12 and methyl orange using graphene oxide as an adsorbent from aqueous phase", ***Chemical Engineering Journal***, Vol. 284, (2016), 687-697. DOI: 10.1016/j.cej.2015.08.131.
55. Akl, M.A.A., "Efficient removal of phenol from water samples using sugarcane bagasse based activated carbon", ***Journal of Analytical & Bioanalytical Techniques***, Vol. 5, No. 2, (2014). DOI: 10.4172/2155-9872.1000189.
56. Momenzadeh, H., Tehrani-Bagha, A.R., Khosravi, A., Gharanjig, K. and Holmberg, K., "Reactive dye removal from wastewater using a chitosan nanodispersion", ***Desalination***, Vol. 271, No. 1-3, (2011), 225-230. DOI: 10.1016/j.desal.2010.12.036..
57. Lai, K.C., Hiew, B.Y.Z., Lee, L.Y., Gan, S., Thangalazhy-Gopakumar, S., Chiu, W.S. and Khiew, P.S., "Ice-templated graphene oxide/chitosan aerogel as an effective adsorbent for sequestration of metanil yellow dye", ***Bioresource Technology*** Vol. 274, (2019), 134-144. DOI: 10.1016/j.biortech.2018.11.048.
58. Costa, T.d.S., Rogez, H. and Pena, R.d.S., "Adsorption capacity of phenolic compounds onto cellulose and xylan", ***Food Science and Technology (Campinas)***, Vol. 35, No. 2, (2015), 314-320. DOI: 10.1590/1678-457x.6568.

Persian Abstract

چکیده

کیتوزان و سلولز فراوانترین بیوپلیمرهایی هستند که می توانند برای حذف رنگ های خطرناک استفاده شوند. با استفاده از TiO2 بر روی ماتریس سلولز- کیتوزان ، تحقیق ما با هدف دستیابی به حذف بالا متانیل زرد با استفاده از مکانیسم جذب هم افزایی / تجزیه نوری ، انجام شده است. ذرات سلولز برای بدست آوردن سلولز مشتق شده از چمن وحشی (Imperata cylindrica L.)استخراج شد. برای تهیه TiO2 / GC / CH از روش ترکیبی ساده استفاده شد که در آن ترکیب با روش توزین ساده افزودنی تعیین شد. TiO2 / GC / CH با استفاده از آزمون مقاومت کششی (همچنین برای SAW نیز استفاده می شود) ، مادون قرمز تبدیل فوریه (FT-IR، پراش اشعه X (XRD) ، کالریمتری اسکن دیفرانسیل (DSC) و میکروسکوپ الکترونی روبشی (SEM)حذف متانیل زرد با استفاده از TiO2 / GC / CH در محدوده pH اسیدی بسیار خوب عمل می کند. حذف به دنبال مدل های شبه نظم جنبشی مرتبه دوم ۰.۹۹۷ (R2)و ایزوترم لانگمویر۰.۹۹۸ (R2)می باشد. qm زیاد حاصل از حذف متانیل زرد تحت تابش اشعه ماورا بنفش (qm = 171.5266)هم افزایی بین جذب و تجزیه نوری را اثبات می کند. TiO2 / GC / CH توسعه یافته می تواند به طور بالقوه در تصفیه فاضلاب برای حذف رنگ آزو استفاده شود.